exit gates are thus unable to mediate sister chromatid cohesion.

Conclusion

It has long been postulated that cohesin forms rings that can be opened to mediate entry and exit of DNA. Here, we used electron microscopy to demonstrate the existence of such open forms, generated either by proteolytic cleavage of Scc1 (mimicking the effect of separase at the metaphase-to-anaphase transition) or by weakening the interaction between Scc1's NHD and the coiled coil of Smc3 (mimicking the opening of cohesin's DNA exit gate). Because the latter is thought to be achieved by Wapl, our exit gate mutant may resemble an otherwise transient intermediate in the ring opening and closure cycle (Fig. 5D). We identified residues at the outside of the solenoid-like Pds5B that reside in direct proximity to Wapl and the Smc3-Scc1 interaction interface (fig. S13), implying that Wapl and Pds5 control the exit gate through direct interactions. However, it remains to be addressed at a mechanistic level how Wapl promotes ring opening and how this is coordinated by Pds5, antagonized by sororin, and regulated by phosphorylation events.

REFERENCES AND NOTES

1. S. Remeseiro, A. Losada, *Curr. Opin. Cell Biol.* **25**, 63–71 (2013).
2. C. H. Haering, J. Löwe, A. Hochwagen, K. Nasmyth, *Mol. Cell* **9**, 773–788 (2002).
3. D. E. Anderson, A. Losada, H. P. Erickson, T. Hirano, *J. Cell Biol.* **156**, 419–424 (2002).
4. S. Gruber, C. H. Haering, K. Nasmyth, *Cell* **112**, 765–777 (2003).
5. C. H. Haering, A. M. Farcas, P. Arumugam, J. Metson, K. Nasmyth, *Nature* **454**, 297–301 (2008).
6. R. Ciosk *et al.*, *Mol. Cell* **5**, 243–254 (2000).
7. P. Arumugam *et al.*, *Curr. Biol.* **13**, 1941–1953 (2003).
8. S. Weitzer, C. Lehane, F. Uhlmann, *Curr. Biol.* **13**, 1930–1940 (2003).
9. S. Gruber *et al.*, *Cell* **127**, 523–537 (2006).
10. J. Buheitel, O. Stemmann, *EMBO J.* **32**, 666–676 (2013).
11. F. Uhlmann, F. Lottspeich, K. Nasmyth, *Nature* **400**, 37–42 (1999).
12. S. Hauf, I. C. Waizenegger, J. M. Peters, *Science* **293**, 1320–1323 (2001).
13. R. Gandhi, P. J. Gillespie, T. Hirano, *Curr. Biol.* **16**, 2406–2417 (2006).
14. S. Kueng *et al.*, *Cell* **127**, 955–967 (2006).
15. A. Tedeschi *et al.*, *Nature* **501**, 564–568 (2013).
16. K. L. Chan *et al.*, *Cell* **150**, 961–974 (2012).
17. C. S. Eichinger, A. Kurze, R. A. Oliveira, K. Nasmyth, *EMBO J.* **32**, 656–665 (2013).
18. P. J. Gillespie, T. Hirano, *Curr. Biol.* **14**, 1598–1603 (2004).
19. T. S. Takahashi, P. Yiu, M. F. Chou, S. Gygi, J. C. Walter, *Nat. Cell Biol.* **6**, 991–996 (2004).
20. A. Kurze *et al.*, *EMBO J.* **30**, 364–378 (2011).
21. K. Shintomi, T. Hirano, *Genes Dev.* **23**, 2224–2236 (2009).
22. N. Zhang *et al.*, *PLOS ONE* **8**, e69458 (2013).
23. Z. Ouyang *et al.*, *Proc. Natl. Acad. Sci. U.S.A.* **110**, 11355–11360 (2013).
24. C. H. Haering *et al.*, *Mol. Cell* **15**, 951–964 (2004).
25. F. Bürmann *et al.*, *Nat. Struct. Mol. Biol.* **20**, 371–379 (2013).
26. P. Arumugam, T. Nishino, C. H. Haering, S. Gruber, K. Nasmyth, *Curr. Biol.* **16**, 1998–2008 (2006).
27. M. A. Deardorff *et al.*, *Nature* **489**, 313–317 (2012).
28. D. Gerlich, B. Koch, F. Dupeux, J. M. Peters, J. Ellenberg, *Curr. Biol.* **16**, 1571–1578 (2006).

ACKNOWLEDGMENTS

We thank O. Hudecz, K. Mechtler, G. Schmauss, K. Uzunova, M. Brandstetter, H. Kotisch, G. Resch, and A. Schleiffer for excellent technical support and I. Berger for an introduction to MultiBac. P.J.H. was supported by the Austrian Science Fund (W1221) and received funding from the European Community (FP7/2007-2013, no. 227764). Research in the laboratory of J.-M.P. is supported by Boehringer Ingelheim, the Austrian Science Fund (SFB-F34 and Wittgenstein award), the Austrian Research Promotion Agency (FFG Laura Bassi), the Vienna Science and Technology Fund (WWTF LS09-13), and the European Community (FP7/2007-2013, no. 241548, MitoSys).

SUPPLEMENTARY MATERIALS

www.sciencemag.org/content/346/6212/968/suppl/DC1
Materials and Methods
Figs. S1 to S13
Tables S1 and S2
References (*29*–*49*)

3 June 2014; accepted 26 September 2014
10.1126/science.1256904

REPORTS

OPTICS

Single-mode laser by parity-time symmetry breaking

Liang Feng,[1]* Zi Jing Wong,[1]* Ren-Min Ma,[1]* Yuan Wang,[1,2] Xiang Zhang[1,2]†

Effective manipulation of cavity resonant modes is crucial for emission control in laser physics and applications. Using the concept of parity-time symmetry to exploit the interplay between gain and loss (i.e., light amplification and absorption), we demonstrate a parity-time symmetry–breaking laser with resonant modes that can be controlled at will. In contrast to conventional ring cavity lasers with multiple competing modes, our parity-time microring laser exhibits intrinsic single-mode lasing regardless of the gain spectral bandwidth. Thresholdless parity-time symmetry breaking due to the rotationally symmetric structure leads to stable single-mode operation with the selective whispering-gallery mode order. Exploration of parity-time symmetry in laser physics may open a door to next-generation optoelectronic devices for optical communications and computing.

Laser cavities support a large number of closely spaced modes because their dimensions are typically much larger than an optical wavelength. As a result, the outputs from such lasers are subject to random fluctuations and instabilities because of mode competition for limited gain. During recent decades, effective mode manipulation and selection strategies have been intensively explored to achieve single-mode operation with both spatial and spectral controllability—a requirement for enhanced laser performance with higher monochromaticity, less mode competition, and better beam quality. Obtaining single-mode operation depends on sufficiently modulated gain and loss, but such modulation is impeded by factors such as inhomogeneous gain saturation. Several approaches have been developed that make use of an additional cavity for the intracavity feedback (*1*), distributed feedback gratings (*2*), an enlarged free spectral range through mode size reduction (*3*, *4*), or spatially varied optical pumping (*5*). However, these approaches are applicable to specific configurations; what is desired is a general design concept with flexible control of cavity modes.

Recent explorations of parity-time (PT) symmetry offer an opportunity to advance laser science by strategically manipulating gain and loss in order to control light transport. PT symmetry was initially proposed in quantum mechanics as an alternative criterion for non-Hermitian Hamiltonians $\hat{H}^{+} \neq \hat{H}$ that possesses a real eigenspectrum (*6*). Because of the equivalence between the Schrödinger equation in quantum mechanics and the electromagnetic wave equation, optics has become an ideal platform for studying the fundamentals of PT symmetry (*7*–*16*), with non-Hermiticity denoted by optical gain and loss. An intriguing PT phase transition has been demonstrated (*11*, *12*), enabling unique optical phenomena such as unidirectional light transport (*13*–*15*) and novel devices including low-power optical diodes (*16*). The strategic modulation of gain and loss in the PT symmetry–breaking condition can fundamentally broaden optical science at both semiclassical and quantum levels (*17*–*23*).

Using the PT symmetry–breaking concept, we delicately manipulated the gain and loss of a microring resonator and observed single-mode laser oscillation of a whispering-gallery mode (WGM). We exploited the continuous rotational symmetry of the microring structure to facilitate unique

[1]NSF Nanoscale Science and Engineering Center, University of California, Berkeley, CA 94720, USA. [2]Materials Sciences Division, Lawrence Berkeley National Laboratory, Berkeley, CA 94720, USA.
*These authors contributed equally to this work. †Corresponding author. E-mail: xiang@berkeley.edu

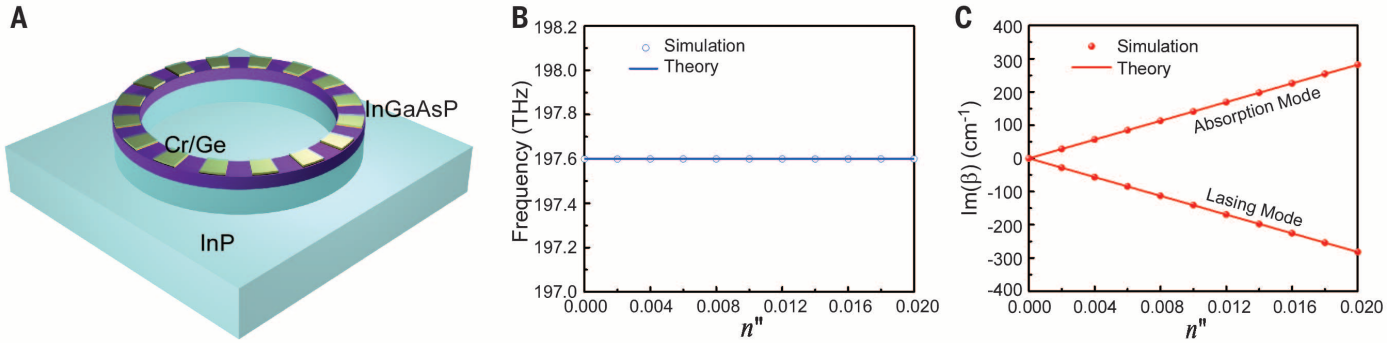

Fig. 1. Design of PT microring lasers. (**A**) Schematic of the PT microring laser, which consists of Cr/Ge bilayer structures arranged periodically in the azimuthal direction on top of the InGaAsP/InP microring resonator to mimic a pure gain/loss modulation. The diameter and width of the microring resonator are 8.9 μm and 900 nm, respectively. The microring also extends 1 μm deeper into the InP substrate. Here, the designed azimuthal order is m = 53 to achieve the resonant wavelength around 1500 nm. (**B** and **C**) The same eigenfrequency (197.6 THz) and complex conjugate imaginary eigenspectra for the two modes at m = 53 determined by numerical simulations (circles and dots) and theoretical calculations (solid lines). The onset in (C) indicates thresholdless PT symmetry breaking.

thresholdless PT symmetry breaking. This thresholdless PT symmetry breaking was valid only for the desired WGM order and enabled two energy-degenerate modes—the non-oscillating loss mode and the oscillating gain mode—whereas all other WGM modes experienced balanced gain/loss modulation and thus remained below the lasing threshold, leading to single-mode lasing.

The PT-synthetic microring resonator was designed with 500-nm-thick InGaAsP multiple quantum wells (MQWs) on an InP substrate (Fig. 1A). InGaAsP MQWs have a high material gain coefficient (>1000 cm^{-1}) around 1500 nm (*24*). The gain/loss modulation, satisfying an exact PT symmetry operation, was periodically introduced using additional Cr-Ge structures on top of the InGaAsP MQW along the azimuthal direction (φ):

$$\Delta n = \begin{cases} n_{\text{gain}} = -in'' \left[\frac{l\pi}{m} < \varphi < \frac{(l+1/2)\pi}{m}\right] \\ n_{\text{loss}} = in'' \left[\frac{(l+1/2)\pi}{m} < \varphi < \frac{(l+1)\pi}{m}\right] \end{cases} \quad (1)$$

where n'' denotes the index modulation in only the imaginary part; m is the azimuthal order of the desired WGM in the microring; and l = 0, 1, 2, ..., $2m$ – 1 divides the microring into $2m$ periods (i.e., $4m$ sections of gain and loss in total). The PT modulation is designed using bilayers on top of the gain material that introduces loss and exactly reverses the sign of the imaginary part of the local modal index while maintaining the same real part (in practice, the deposition of Cr/Ge also slightly modifies the real part on the order of 0.01%). The wave numbers of the eigenmodes in our PT microring resonator are $\beta = \beta_0 \pm i\kappa n''$, where β_0 is the intrinsic wave number of the WGM without gain or loss, and κ denotes the coupling between the clockwise and counterclockwise traveling waves through PT modulation in the microring resonator (*25*) (see supplementary text). Evolution of PT symmetry of the m = 53 WGM in the microring resonator as a function of imaginary part–index modulation can be seen from the corresponding

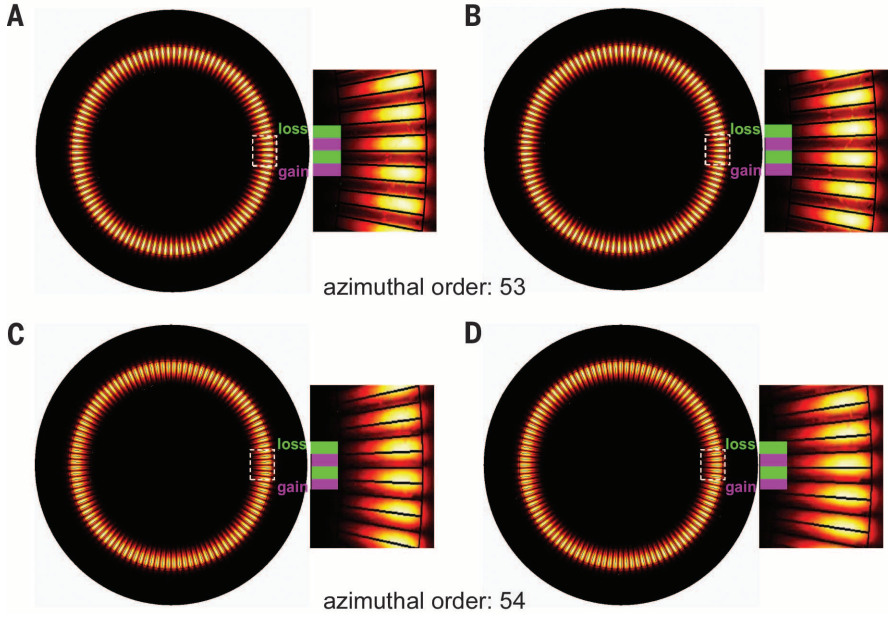

Fig. 2. WGMs of different azimuthal orders in the PT microring laser. (**A** and **B**) Eigen–electric field intensity distributions of paired lasing and absorption modes at m = 53. Fields are confined in the gain (A) and loss (B) sections, resulting in conjugate modal gain/loss coefficients: effective gain of 268 cm^{-1} [Im(β) = –134 cm^{-1}] for the lasing mode (A) and effective loss of –268 cm^{-1} [Im(β) = 134 cm^{-1}] for the absorption mode (B). (**C** and **D**) Eigen–electric field intensity distributions of paired WGMs at m = 54. The two modes share the same eigenfrequency of 200.9 THz and a similar modal loss coefficient of –8 cm^{-1} [Im(β) = 4 cm^{-1}].

complex eigenspectra (Fig. 1, B and C). Two WGMs are energy-degenerate at the same resonant eigenfrequency, but their modal wave numbers are complex conjugates of each other, corresponding to PT symmetry breaking with a simultaneous coexistence of lasing and absorption eigenmodes.

The microring resonator goes into the PT-broken phase with a bifurcation in the imaginary spectrum even if the strength of gain/loss modulation is infinitesimal. This thresholdless feature in our PT phase transition is attributable to the continuous rotational symmetry associated with the desired WGM order in the absence of a real-index modulation (see supplementary text and fig. S1). This feature is distinct from the previously studied coupled PT waveguide systems, including the recently developed coupled gain/loss WGM resonators (*16*, *23*). In those systems, there are no continuous symmetries, such that PT symmetry breaking requires a finite strength of the gain/loss modulation (*20*). Although our design is based on a linear model by assuming a steady lasing state with a certain gain coefficient of InGaAsP (*3*, *4*, *19*, *21*, *26*), it is worth noting that lasing itself is an intrinsic nonlinear process. However, this thresholdless PT symmetry breaking in our system is robust against optical nonlinearity and its induced PT phase transition (*10*). In the experiment, a slight deviation from the desired perfectly balanced gain/loss modulation

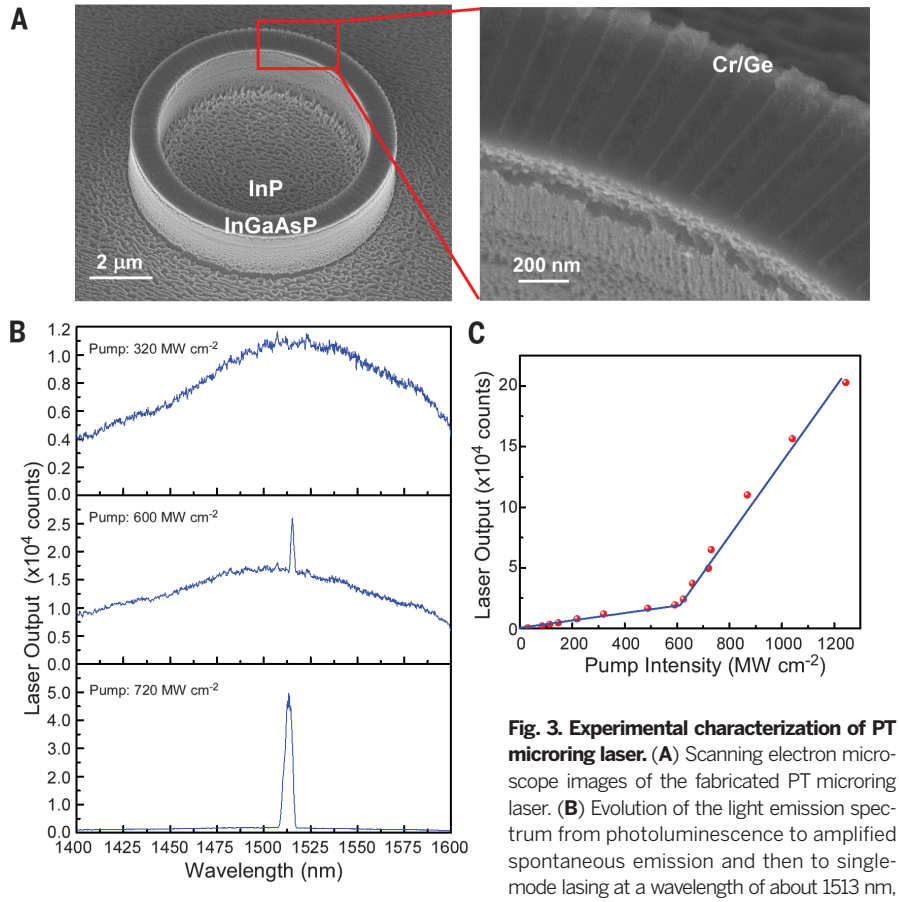

Fig. 3. Experimental characterization of PT microring laser. (**A**) Scanning electron microscope images of the fabricated PT microring laser. (**B**) Evolution of the light emission spectrum from photoluminescence to amplified spontaneous emission and then to single-mode lasing at a wavelength of about 1513 nm, shown as the peak power density of pump light was increased from 320 MW cm^{-2} to 600 MW cm^{-2} and then to 720 MW cm^{-2}. (**C**) Light-light curve of the PT microring laser shows the power relationship between the lasing emission and the pump light. A clear onset of the intrinsic single-mode lasing appears at a threshold slightly larger than 600 MW cm^{-2}.

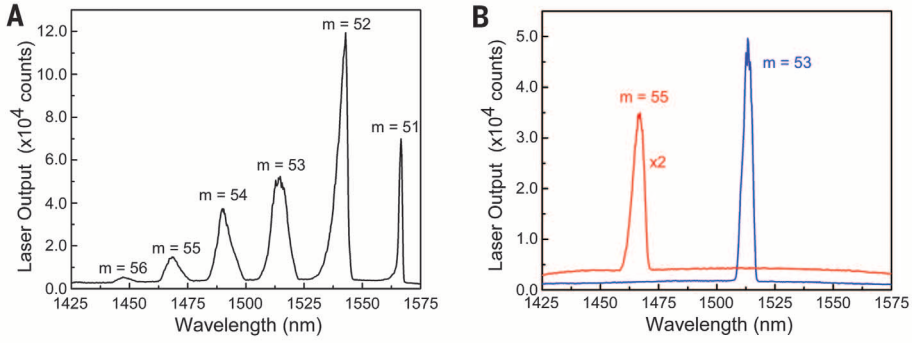

Fig. 4. Comparison between PT laser and typical microring laser. (**A**) Multimode lasing spectrum observed from the typical microring WGM laser, showing a series of lasing modes corresponding to different azimuthal orders. (**B**) Single-mode lasing spectra of the PT microring lasers operating at the m = 53 and m = 55 azimuthal orders, consistent with the lasing wavelength for the same azimuthal orders in (A). This confirms that our PT microring laser does not alter original WGMs but efficiently selects the desired lasing mode.

is possible, but the thresholdless PT symmetry–breaking feature is still preserved (see supplementary text and fig. S2).

Figure 2, A and B, shows the modal intensity distribution of the lasing and absorption modes in the PT microring resonator with 15 nm of Cr and 40 nm of Ge on top (corresponding to the InGaAsP MQW material gain coefficient of 800 cm^{-1} for the presumed ideal balanced gain/loss modulation). In the lasing mode, electric fields are confined mainly in the amplification sections, exhibiting a net modal gain coefficient of 268 cm^{-1}, whereas the absorption mode is loss-dominant with electric fields mainly under the Cr/Ge sections, with a loss coefficient of −268 cm^{-1}. Their eigenfrequencies are energy-degenerate but their gain/loss coefficients are opposite one another, consistent with the features of PT symmetry breaking. For other WGMs, for instance m = 54, electric fields in both energy-degenerate WGMs are uniformly distributed in gain and loss regimes. As a result, gain and loss are averaged out, creating modal wave numbers without net gain or loss (simulations show both modes have a similarly small loss coefficient of about −8 cm^{-1}) (Fig. 2, C and D). In this case, WGMs fall into the PT symmetric phase for the nondesired azimuthal orders (see supplementary text). It is therefore clear that only the lasing mode at the desired order contains a positive effective gain coefficient above the lasing threshold, enabling single-mode lasing. All other WGMs are suppressed by the intentionally introduced loss from the PT modulation. This unique single-mode operation is valid even with an arbitrarily wide gain spectrum because of its stringent mode selectivity, which is inherently different from the conventional single-mode microring lasers that use real-index coupling and modulation to achieve the mode splitting in eigenfrequencies and are limited by the bandwidth of the gain media (*27*, *28*).

The PT microring laser with Cr/Ge modulations (Fig. 3A) was fabricated using overlay electron beam lithography and plasma etching. Under optical pumping with a femtosecond laser (see supplementary text and fig. S3), a broad photoluminescence emission around 1500 nm was first observed at low pump power densities. As the pump power was increased, the transition to amplified spontaneous emission and full laser oscillation was clearly observed from the rapidly increasing spectral purity of the cavity mode (Fig. 3B). At higher pumping intensities well above the lasing threshold, the single-mode lasing peak is seen at the wavelength of 1513 nm, confirming our theoretical prediction of the single WGM lasing operation of the PT microring laser. The lasing linewidth is about 1.7 nm around the transparency pump power, corresponding to a quality factor of about 890 that is limited by the surface roughness of the sample. In Fig. 3C, the light-light curve corresponding to single-mode emission clearly shows a slope change corresponding to a lasing threshold at peak pump power density of about 600 MW cm^{-2}. The lasing mode (m = 53) in the PT-broken phase emerges above the lasing threshold, creating pronounced single-mode lasing with an extinction ratio of more than 14 dB, whereas other WGMs are all below the lasing threshold and are strongly suppressed.

For comparison, a control sample of a WGM laser was fabricated consisting of the same-sized InGaAsP/InP microring resonator without additional Cr/Ge index modulation. As expected, we observed a typical multimode lasing spectrum with different WGM azimuthal orders distributed over the gain spectral region (Fig. 4A). Relative to the PT microring laser, it can be seen that

under a similar pumping condition, the resonance peak for the same azimuthal order of m = 53 well matches the single-mode lasing of the PT ring resonator at a wavelength of 1513 nm (Fig. 4B). The power efficiency and the lasing threshold are also similar because the introduced loss in the PT microring laser minimally affects the desired lasing mode. We also fabricated an additional PT microring laser with a different azimuthal PT modulation for the order of m = 55. Its lasing emission at 1467 nm (Fig. 4B) also agrees well with the multimode lasing spectrum of the conventional WGM laser for the same azimuthal order (Fig. 4A). It is evident that instead of altering the WGM in the microring resonator, the introduced PT gain/loss modulation selects the lasing WGM in the PT-broken phase over a broad spectral band. By changing the desired azimuthal order of the structured PT modulation, the single-mode lasing frequency can be efficiently selected. Although we demonstrated lasing for only two WGM orders, this mode selection concept is general and in principle valid for arbitrary gain spectra. In applications, the demonstrated stable single-mode lasing can be efficiently routed, using a bus waveguide through the evanescent ring-waveguide coupling, to photonic integrated circuits for on-chip signal amplification and processing.

We have demonstrated a PT microring laser by delicate exploitation of optical loss and gain. Such a microring laser is intrinsically single-mode regardless of the gain spectral bandwidth. This is because the continuous rotational symmetry of PT modulation enables the thresholdless PT symmetry breaking only for the desired mode. More important, our PT laser demonstration is a major step toward unique photonic devices such as a PT-symmetric laser-absorber that coincides lasing and anti-lasing [i.e., coherent perfect absorption (*29*, *30*)] simultaneously.

REFERENCES AND NOTES

1. D. C. Hanna, B. Luther-Davies, R. C. Smith, *Electron. Lett.* **8**, 369 (1972).
2. H. Ghafouri-Shiraz, *Distributed Feedback Laser Diodes and Optical Tunable Filters* (Wiley, New York, 2003).
3. M. T. Hill *et al.*, *Nat. Photonics* **1**, 589–594 (2007).
4. R. M. Ma, R. F. Oulton, V. J. Sorger, G. Bartal, X. Zhang, *Nat. Mater.* **10**, 110–113 (2011).
5. S. F. Liew, B. Redding, L. Ge, G. S. Solomon, H. Cao, *Appl. Phys. Lett.* **104**, 231108 (2014).
6. C. M. Bender, S. Böttcher, *Phys. Rev. Lett.* **80**, 5243–5246 (1998).
7. K. G. Makris, R. El-Ganainy, D. N. Christodoulides, Z. H. Musslimani, *Phys. Rev. Lett.* **100**, 103904 (2008).
8. S. Klaiman, U. Günther, N. Moiseyev, *Phys. Rev. Lett.* **101**, 080402 (2008).
9. A. E. Miroshnichenko, B. A. Malomed, Y. S. Kivshar, *Phys. Rev. A* **84**, 012123 (2011).
10. Y. Lumer, Y. Plotnik, M. C. Rechtsman, M. Segev, *Phys. Rev. Lett.* **111**, 263901 (2013).
11. A. Guo *et al.*, *Phys. Rev. Lett.* **103**, 093902 (2009).
12. C. E. Rüter *et al.*, *Nat. Phys.* **6**, 192–195 (2010).
13. Z. Lin *et al.*, *Phys. Rev. Lett.* **106**, 213901 (2011).
14. A. Regensburger *et al.*, *Nature* **488**, 167–171 (2012).
15. L. Feng *et al.*, *Nat. Mater.* **12**, 108–113 (2013).
16. B. Peng *et al.*, *Nat. Phys.* **10**, 394–398 (2014).
17. H. Schomerus, *Phys. Rev. Lett.* **104**, 233601 (2010).
18. G. Yoo, H. S. Sim, H. Schomerus, *Phys. Rev. A* **84**, 063833 (2011).
19. S. Longhi, *Phys. Rev. A* **82**, 031801(R) (2010).
20. Y. D. Chong, L. Ge, A. D. Stone, *Phys. Rev. Lett.* **106**, 093902 (2011).
21. M.-A. Miri, P. LiKamWa, D. N. Christodoulides, *Opt. Lett.* **37**, 764–766 (2012).
22. M. Liertzer *et al.*, *Phys. Rev. Lett.* **108**, 173901 (2012).
23. M. Brandstetter *et al.*, *Nat. Commun.* **5**, 4034 (2014).
24. M. Körbl, A. Gröning, H. Schweizer, J. L. Gentner, *J. Appl. Phys.* **92**, 2942 (2002).
25. J. Wiersig, S. W. Kim, M. Hentschel, *Phys. Rev. A* **78**, 053809 (2008).
26. A. Mizrahi *et al.*, *Opt. Lett.* **33**, 1261–1263 (2008).
27. L. Shang, L. Liu, L. Xu, *Opt. Lett.* **33**, 1150–1152 (2008).
28. A. Arbabi, Y. M. Kang, C. Y. Lu, E. Chow, L. L. Goddard, *Appl. Phys. Lett.* **99**, 091105 (2011).
29. Y. D. Chong, L. Ge, H. Cao, A. D. Stone, *Phys. Rev. Lett.* **105**, 053901 (2010).
30. W. Wan *et al.*, *Science* **331**, 889–892 (2011).

ACKNOWLEDGMENTS

Supported by Office of Naval Research Multidisciplinary University Research Initiative program grant N00014-13-1-0649. We thank Y.-L. Xu and K. O'Brien for helpful discussions.

SUPPLEMENTARY MATERIALS

www.sciencemag.org/content/346/6212/972/suppl/DC1
Supplementary Text
Figs. S1 to S3

8 July 2014; accepted 17 October 2014
Published online 30 October 2014;
10.1126/science.1258479

OPTICS

Parity-time–symmetric microring lasers

Hossein Hodaei, Mohammad-Ali Miri, Matthias Heinrich,* Demetrios N. Christodoulides, Mercedeh Khajavikhan†

The ability to control the modes oscillating within a laser resonator is of fundamental importance. In general, the presence of competing modes can be detrimental to beam quality and spectral purity, thus leading to spatial as well as temporal fluctuations in the emitted radiation. We show that by harnessing notions from parity-time (PT) symmetry, stable single–longitudinal mode operation can be readily achieved in a system of coupled microring lasers. The selective breaking of PT symmetry can be used to systematically enhance the maximum attainable output power in the desired mode. This versatile concept is inherently self-adapting and facilitates mode selectivity over a broad bandwidth without the need for other additional intricate components. Our experimental findings provide the possibility to develop synthetic optical devices and structures with enhanced functionality.

Since the early days of the laser, enforcing single-mode operation in a given arrangement has been one of the primary goals of cavity design (*1*). At first glance, one might expect these challenges to become less acute in the course of miniaturization, as the separation of resonances, or free spectral range, scales inversely with size. However, despite their smaller size, mode management in semiconductor lasers is still demanding because of their large inhomogeneously broadened gain bandwidth (*2*). In such broadband gain environments, the lasing of the desired mode does not prevent the neighboring resonances from also experiencing amplification. Consequently, additional steps must be taken to suppress the competing parasitic modes. This can be accomplished in a number of ways, as, for example, coupling to detuned external cavities (*3*), by including intracavity dispersive elements such as distributed feedback gratings or distributed Bragg mirrors (*4*–*6*), by spatially modulating the pump (*7*), or more recently by extreme confinement of light in subwavelength structures using metallic cavities (*8*–*10*). However, not all of these schemes are practically compatible with every type of resonator, and each of them introduces further demands in terms of design complexity and fabrication tolerances. Clearly, of importance will be to identify alternative strategies through which mode selection can be established not only in a versatile manner, but also without any negative impact on the overall efficiency.

A prominent class of integrated laser arrangements is based on microring resonators (*11*, *12*). By virtue of their high refractive index contrast, such configurations can support whispering gallery modes that exhibit high quality factors and small footprints, thus making them excellent candidates for on-chip integrated photonic applications. However, like many other microscale resonators, these cavities tend to support multiple longitudinal modes with almost similar quality factors throughout their gain bandwidth, while offering little control in terms of mode discrimination with conventional techniques.

CREOL, The College of Optics and Photonics, University of Central Florida, Orlando, FL 32816-2700, USA.
*Present address: Institute of Applied Physics, Abbe Center of Photonics, Friedrich-Schiller-Universität Jena, Max-Wien-Platz 1, 07743 Jena, Germany. **†Corresponding author. E-mail: mercedeh@creol.ucf.edu**